Novel Model of Constrictive Pericarditis Associated With Autoimmune Heart Disease in Interferon-γ–Knockout Mice

Marina Afanasyeva, MD, MPH, PhD*; Dimitrios Georgakopoulos, PhD*; DeLisa Fairweather, PhD; Patrizio Caturegli, MD; David A. Kass, MD; Noel R. Rose, MD, PhD

Background—Constrictive pericarditis represents a serious hemodynamic syndrome that may lead to heart failure. Studies of its pathophysiological mechanisms have been impeded by the lack of an animal model.

Methods and Results—Cardiac myosin–induced experimental autoimmune myocarditis in interferon (IFN)-γ–knockout (KO) mice results in increased cardiac inflammation and development of severe grossly detectable pericarditis. Using in vivo pressure-volume studies, we found that the acute phase of experimental autoimmune myocarditis in IFN-γ–KO mice was characterized by reduced left ventricular (LV) volumes compared with wild-type mice. The KO mice exhibited a classic restrictive/constrictive phenotype with decreased cardiac output, increased chamber stiffness, preserved ejection fraction, and impaired diastolic filling, characterized by reduced deceleration time and pressure tracings showing the square root sign similar to that observed in clinical cases of constrictive pericarditis. This phenotype was not associated with the severity of myocarditis but correlated with the presence of grossly detectable adhesive pericarditis present only in the KO group and characterized by increased pericardial inflammation and fibrosis. Comparison of IFN-γ–KO and wild-type mice matched for the severity of myocardial disease further confirmed that pericarditis, and not myocarditis, was responsible for smaller LV volumes, reduced cardiac output, increased cardiac stiffness, and increased peak filling rate adjusted for end-diastolic volumes in KO mice.

Conclusions—Autoimmune heart disease in IFN-γ–KO mice results in increased pericardial inflammation and fibrosis, leading to constrictive phenotype during the acute phase of disease. It represents a novel animal model of constrictive pericarditis. (***Circulation*. 2004;110:2910-2917.**)

Key Words: cardiac output ■ pressure–volume relation ■ hemodynamics ■ inflammation ■ myocarditis

Constrictive pericarditis represents a serious hemodynamic syndrome that may lead to heart failure unless surgically treated.[1] Causes of constrictive pericarditis include infections, such as tuberculosis, open-chest surgery, radiation therapy, malignancies, and autoimmune disorders; however, 40% of all cases remain idiopathic.[2,3] Pericarditis of autoimmune etiology may result from an ongoing inflammatory process involving other layers of the heart, particularly the myocardium. Examples of an inflammatory/autoimmune involvement of >1 cardiac layer include rheumatic pancarditis and viral perimyocarditis.

A better understanding of the etiology and pathogenesis of constriction associated with the pericardial disease is critical for prevention, early diagnosis, and treatment of this condition. However, studies on the mechanisms of development of constrictive pericarditis have been impeded by the lack of an animal model. In this work we present a novel mouse model of constrictive pericarditis associated with autoimmune heart disease in the context of interferon (IFN)-γ deficiency. IFN-γ–knockout (KO) mice immunized with cardiac myosin (CM) demonstrated gross and histological features of pericarditis. In vivo hemodynamic analysis revealed classic restrictive/constrictive physiology associated with pericarditis in the KO mice. Thus, IFN-γ–KO mice present a model to study the mechanisms of pericardial remodeling and its effects on hemodynamics and the interplay between myocardial and pericardial disease, and they provide insights into the protective role of IFN-γ in the development of pericardial inflammation and fibrosis.

Methods

Mice

Experimental autoimmune myocarditis (EAM) was induced in 10- to 12-week old female wild-type (WT) and IFN-γ–KO BALB/c

Received June 9, 2004; revision received August 5, 2004; accepted August 11, 2004.

From the Department of Pathology (M.A., D.F., P.C., N.R.R.), Department of Medicine (D.G., D.A.K.), and W. Harry Feinstone Department of Molecular Microbiology and Immunology (N.R.R.), Johns Hopkins Medical Intitutions, Baltimore, Md.

*The first 2 authors contributed equally to this work.

Correspondence to Marina Afanasyeva, MD, MPH, PhD, or Dimitrios Georgakopoulos, PhD, University of Calgary, Cardiovascular Research Group, Faculty of Medicine, 3330 Hospital Dr NW, Health Sciences Centre, Room 1640, Calgary AB T2N 4N1, Alberta, Canada. E-mail afanasym@ucalgary.ca or dgeorgak@ucalgary.ca

Circulation **is available at http://www.circulationaha.org** **DOI: 10.1161/01.CIR.0000147538.92263.3A**

Hemodynamic Features of Constrictive Pericarditis in IFN-γ–KO Mice in EAM

	Control		Acute Myocarditis		
				KO	
Parameter	WT (n=6)	KO (n=4)	WT (n=9)	No Pericarditis (n=5)	Pericarditis (n=6)
HW, mg	96.7±4.5	113.3±10.7	116.6±19.2	125.8±14.8	186.0±38.6*†
HW/BW, mg×g^{-1}	4.3±0.5	4.6±0.4	5.3±0.6	5.6±0.7	10.0±3.0*†
HR, min^{-1}	584.4±17.3	558.0±41.9	655.8±35.2	629.6±82.0	643.5±16.1
CO, mL×min^{-1}	13.1±1.3	11.2±0.5	12.5±1.4	8.7±0.8*	5.1±0.9*†
EDV, μL	35.5±3.4	33.9±5.9	35.1±7.4	27.2±7.2*	16.0±3.9*†
ESP, mm Hg	113.7±9.0	119.2±3.5	110.4±5.8	105.8±2.2	93.9±13.8*†
EDP, mm Hg	8.2±2.6	8.4±3.1	8.6±3.5	10.1±1.7	11.9±3.1
EF	0.63±0.08	0.60±0.06	0.56±0.12	0.54±0.15	0.52±0.16
dP/dt_{max}, mm Hg×s^{-1}	14 587.2±1363.3	15 375.8±1279.9	15 121.5±2087.3	12 249.3±1513.9*	9642.2±3459.2*
dP/dt_{max}/EDV, mm Hg×s^{-1}×μL^{-1}	339.1±74.8	381.1±12.5	366.6±83.3	494.7±287.9	536.9±165.2*
$Power_{max}$, W	11.2±2.6	11.1±1.2	10.3±1.9	7.8±1.5*	4.5±0.8*†
PRSW, mm Hg	76.3±8.3	72.8±8.5	73.9±10.5	76.3±25.1	64.5±7.9
Ees, mm Hg×μL^{-1}	2.8±0.8	3.0±1.2	3.6±1.1	4.6±1.3	7.6±2.2*†
τ, ms	3.5±0.2	3.4±0.4	3.5±0.6	3.6±0.3	5.0±1.2*†
PFR/EDV, s^{-1}	36.7±10.3	37.3±9.6	39.3±10.2	21.2±6.9*	21.6±5.4*
Time to PFR, ms	22.3±1.4	20.6±0.5	19.5±2.5	29.0±7.2	27.2±9.7
Eed, mm Hg×μL^{-1}	0.05±0.01	0.06±0.02	0.16±0.05	0.14±0.09	0.25±0.09*
E_7, mm Hg×μL^{-1}	0.23±0.04	0.23±0.05	0.22±0.05	0.30±0.08	0.53±0.2*†
LVV_7, μL	31.8±5.9	31.4±5.5	32.7±7.3	24.7±6.0	14.3±4.3*†
t_{dec}, ms	26.8±3.7	28.3±1.0	24.3±3.3	25.8±5.6	14.7±2.6*†

Acute myocarditis corresponds to day 21 after immunization. Controls are age-matched unimmunized mice. HW indicates heart weight; HW/BW, ratio of heart weight to body weight; HR, heart rate; CO, cardiac output; ESP, end-systolic pressure; EDP, end-diastolic pressure; EF, ejection fraction; PRSW, preload-recruitable stroke work, which represents stroke work normalized to EDV; Ees, end-systolic elastance; τ, time constant of diastolic relaxation; PFR, peak filling rate; Eed, end-diastolic elastance; E_7, diastolic elastance at filling pressure of 7 mm Hg; and LVV_7, LV volume at filling pressure of 7 mm Hg. Data are mean±SD.

*$P<0.05$ compared with WT mice with myocarditis, Student t test; †$P<0.05$ compared with cases with no pericarditis, Student t test.

mice obtained from the Jackson Laboratory (Bar Harbor, Maine) and maintained in the Johns Hopkins University School of Medicine conventional animal facility. The Animal Care and Use Committee of Johns Hopkins University approved the animal work.

Induction and Histological Assessment of Disease

CM was purified from murine hearts according to the procedure of Shiverick et al.[4] Mice received subcutaneous injections of 200 to 250 μg of CM emulsified in complete Freund's adjuvant (Sigma) on days 0 and 7 and intraperitoneal injection of 500 ng of pertussis toxin on day 0 (List Biological Laboratories). For histological assessment, mice were killed on day 21 after immunization, and hearts were fixed in 10% phosphate-buffered formalin and embedded in paraffin. Sections 5 μm thick were cut from base to apex and stained with hematoxylin and eosin. Every fifth section (total of 5 sections from each heart) was examined by 2 independent investigators in a blinded manner. Severity of myocarditis was assessed on the basis of the percentage of the heart section infiltrated by leukocytes according to the following classification: grade 0, no disease; grade 1, ≤10%; grade 2, 11% to 30%; grade 3, 31% to 50%; grade 4, 51% to 90%; and grade 5, >90%. Presence of pericarditis was assessed by gross examination as well as by histological examination of sections stained with hematoxylin and eosin. Percentages of pericardial and myocardial fibrosis were assessed on heart sections with Masson's trichrome stain with the use of a microscope with a grid and were calculated as follows: (area of fibrosis/total area of a cross section)×100.

Hemodynamic Analysis

Pressure-volume studies were performed by in vivo left ventricular (LV) catheterization in unimmunized and immunized mice on day 21 after immunization as previously described.[5] Anesthesia was initiated with methoxyflurane followed by an intraperitoneal injection of urethane (800 to 1000 mg/kg), etomidate (20 to 30 mg/kg), and morphine (1 to 2 mg/kg). The data were recorded with the use of a 1.4F pressure-volume catheter (SPR-719, Millar Instruments). LV deceleration time (t_{dec}) was calculated as time required for flow to decline from peak flow to zero (E wave). Flow was derived with the use of the first derivative of LV volume signal with respect to time (dV/dt). The time constant of isovolumic relaxation (τ) was derived with the use of the logistic model as described by Matsubara et al.[6]

Statistical Analyses

The data were analyzed with the use of the 2-tailed Student t test. Analysis of an association between a severity score and a hemodynamic parameter was performed with the Spearman rank test. Linear regression analysis was used to assess the association between myocardial and pericardial fibrosis and their effects on hemodynamic parameters. The data were analyzed with the use of SigmaStat 3.01 (SPSS Inc) software. Probability values of ≤0.05 were considered statistically significant.

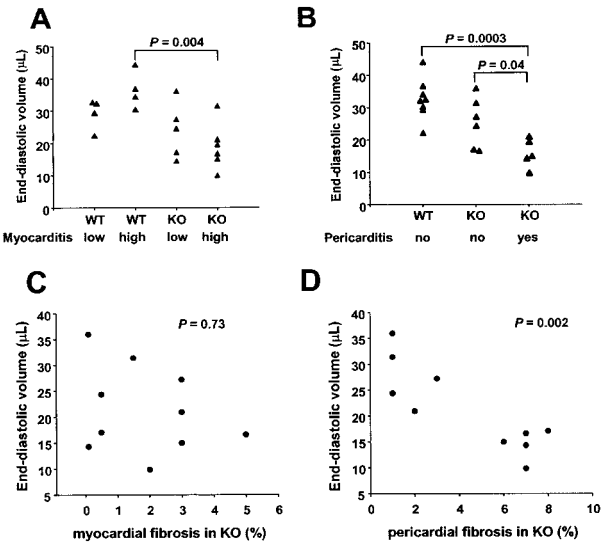

Figure 1. Reduced EDV in IFN-γ–KO mice is associated with presence of pericarditis. A, Absence of association between histological score of myocarditis and EDV in KO mice. Scores <1 are indicated as low, and scores ≥3 are indicated as high. B, Association between presence of gross pericarditis and EDV. C, Absence of association between myocardial fibrosis and EDV in IFN-γ–KO mice. D, Increased pericardial fibrosis in IFN-γ–KO mice results in reduction in EDV. Data are from day 21 after immunization. Each symbol represents an individual mouse. In A and B, probability values are calculated with the use of 2-tailed Student *t* test. In C and D, probability values indicate significance of slope of the regression line.

Results

Constrictive Physiology Associated With Pericarditis

CM-induced EAM in IFN-γ–KO mice is characterized by exaggerated myocardial inflammation.[7,8] We found that the KO mice also develop severe pericarditis. To study how cardiac inflammation in a setting of IFN-γ deficiency affects LV function, we performed in vivo hemodynamic measurements during the acute phase of EAM (day 21 after immunization). IFN-γ–KO mice had significantly lower LV end-diastolic volumes (EDV) than both immunized WT and unimmunized KO mice (Table). Reduced LV volumes did not correlate with the severity of myocarditis in the individual KO mice (Figure 1A). In contrast, in the WT mice higher myocarditis scores were associated with larger EDV, indicative of the progression to dilated cardiomyopathy (Figure 1A).

Reduced LV EDV significantly correlated with the presence of pericarditis on gross examination in the KO mice (Figure 1B). Grossly detectable pericarditis developed only in IFN-γ–KO mice and was characterized by thickened pericardium with white discoloration and adhesions to the surrounding structures (Figure 2A, 2B). IFN-γ–KO mice with acute pericarditis demonstrated a classic restrictive/constrictive phenotype with relatively preserved indices of systolic function (ejection fraction and maximal rate of pressure development [dP/dt_{max}] adjusted for end-diastolic volume [dP/dt_{max}/EDV]), increased end-systolic and end-diastolic elastance, and diastolic dysfunction (Table). Diastolic dysfunction in these mice was characterized by pressure tracings showing the square root sign, similar to that observed in clinical cases of constrictive pericarditis and indicative of an abrupt cessation of filling due to early pressure equalization related to constriction (Figures 2F and 3A, 3B). Volume tracings in Figure 3C further confirm the premature termination of early rapid filling and the onset of diastasis in the KO with pericarditis. At the same point in the cardiac cycle, diastasis begins in KO mice, while WT mice (with either low or high score of myocarditis) are undergoing early filling. Figure 3D provides diastolic pressure-volume tracings for the same mice as in Figure 3C, which show an early and steep rise in pressure with filling in KO mice. This was associated with a significant reduction in t_{dec}[9] compared with both immunized WT and immunized KO mice without pericarditis (Table), consistent with increased diastolic stiffness due to increased pericardial constraint, with most of the filling being accomplished in early diastole. Diastolic relaxation (τ) was also prolonged in the KO mice with pericarditis.

Morbidity Associated With Pericarditis in IFN-γ–KO Mice

During the course of disease, IFN-γ–KO mice had a change in body weight of −10.3% (±13.7%), and WT mice had a change in body weight of 14.0% (±5.7%) relative to day 0. At the time of euthanasia (day 21), the KO mice had significantly lower body weight than the WT mice (17.3±3.6 versus 21.9±2.7 g; $P=0.006$). Body weights were not different between the groups at day 0. Among the KO mice, presence of pericarditis was associated with significantly lower body weight ($P=0.014$) and increased heart weight, resulting in increased ratio of heart weight to body weight (Table). At day 21, in the KO mice body weight was inversely associated with pericardial fibrosis ($P=0.04$) but lacked association with myocardial fibrosis ($P=0.27$).

At euthanasia, KO mice (5/12) but none of the WT mice (0/9) exhibited symptoms of heart failure, including cachexia, reduced physical activity, hyporeflexia, hypothermia, and presence of fluid in the pleural and peritoneal cavities ($P=0.045$, Fisher exact test). Overall, there was no mortality before day 21 in both groups. Among the KO mice with heart failure symptoms (n=5), 3 mice died before or during the surgery and showed gross and histological evidence of severe pericarditis.

Morphological Features of Pericarditis

On gross examination, pericarditis in the KO group appeared as thickened, rigid pericardium with white discoloration, forming adhesions to the surrounding structures, such as the pleura, diaphragm, and chest wall (Figure 2A, 2B). During pressure-volume studies, penetration of the pericardial structures while the catheter was advanced through the apex and into the LV cavity was somewhat impeded in the KO mice compared with the WT mice and required an application of greater force. Histological examination of the hearts confirmed the presence of pericarditis in the KO mice (Figure 4). The observed morphological spectrum of pericarditis included cases with a predominant inflammatory component (Figure 4E, 4F) and cases with a predominant fibrotic

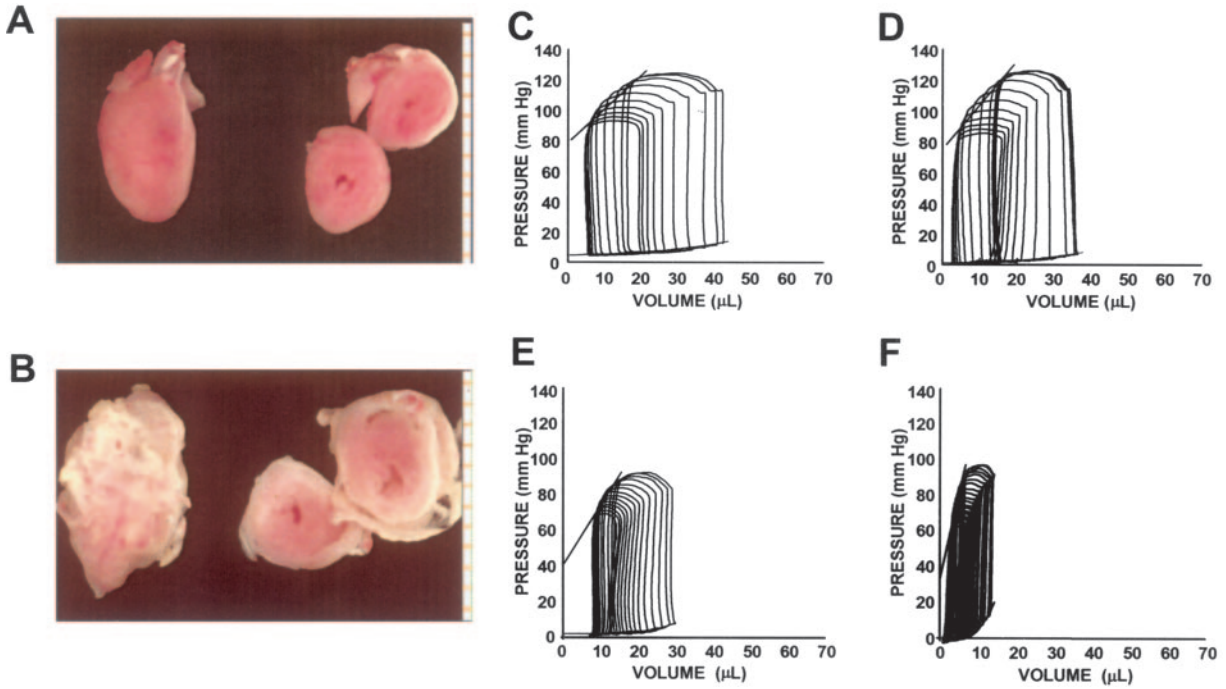

Figure 2. Morphological and functional evidence of constrictive pericarditis in IFN-γ–KO mice. A and B, Representative gross hearts and cross sections from immunized WT (A) and KO (B) mice. C to F, Representative pressure-volume relations from unimmunized WT (C), unimmunized IFN-γ–KO (D), WT with severe myocarditis (E), and IFN-γ–KO mice with severe myocarditis (F). In A, B, E, and F, data were obtained on day 21 after immunization.

component associated with milder inflammation (Figure 4G, 4H). In addition to the mononuclear population, pericardial inflammatory infiltrate was characterized by the presence of polymorphonuclear cells, including eosinophils (Figure 4E, inset), which are typical of inflammatory lesions in IFN-γ–KO mice. Pericarditis in the KO mice was also associated with mesothelial hyperplasia and mesothelial reaction characterized by a change to cuboidal morphology of mesothelial cells, typical of pericardial injury. In addition to the adhesions with the surrounding tissues, there were adhesions between the parietal and visceral layers, leading to the obliteration of the pericardial sac. The WT mice developed mild to no pericardial reaction on histological examination, including those with severe myocarditis (Figure 4C, 4D), and none of them developed grossly detectable pericarditis.

Using Masson's trichrome stain, we found that IFN-γ–KO mice had a significantly greater percentage of pericardial fibrosis than the WT mice and that the extent of pericardial

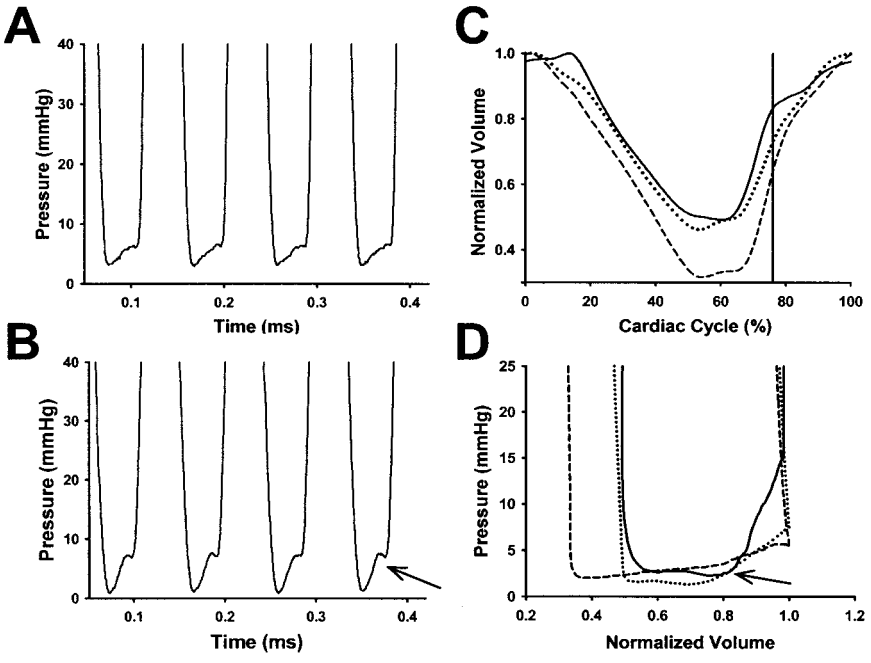

Figure 3. Diastolic dysfunction associated with constrictive pericarditis in IFN-γ–KO mice. A, LV pressure tracing from WT mouse. B, LV pressure tracing from IFN-γ–KO mouse showing a pronounced early dip with a subsequent rapid rise to a plateau (square root sign, arrow) typical of restrictive/constrictive disease. C and D, Volume and pressure-volume tracings, respectively, from IFN-γ–KO mouse with pericarditis (myocarditis score of 2.75; solid line), WT mouse with severe myocarditis (score of 3; dotted line), and WT mouse with mild myocarditis (score of 0.75; dashed line). Note the premature onset of diastasis in the KO mouse compared with both groups of WT mice, as indicated by the vertical line in C. Arrow in D indicates onset of early rapid rise in pressure with filling in the KO mouse. C and D, For comparison purposes, volumes were normalized to EDV. Data are derived with the use of in vivo LV catheterization on day 21 after immunization.

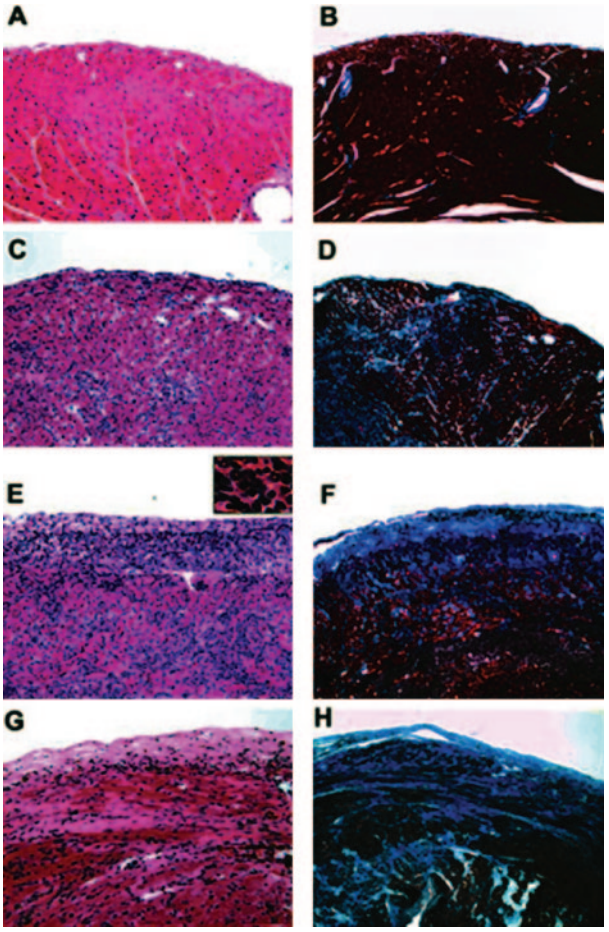

Figure 4. Histological features of pericarditis in IFN-γ–KO mice. A and B, Normal pericardium in unimmunized WT mouse. C and D, Mild infiltration and minimal fibrotic response in the pericardium in WT mouse with severe myocarditis. E and F, Severe pericarditis with strong inflammatory and fibrotic components in IFN-γ–KO mouse with severe myocarditis. Inset in E shows abundant eosinophils in the pericardial infiltrate. G and H, Severe fibrotic pericarditis with a relatively mild inflammatory component in IFN-γ–KO mouse with severe myocarditis. A, C, E, and G, Hematoxylin and eosin stain; magnification ×40. B, D, F, and H, Masson's trichrome stain; magnification ×20. Inset in E, Hematoxylin and eosin stain; magnification ×160.

fibrosis in the KO mice was unrelated to the extent of myocardial fibrosis (Figure 5A, 5C, respectively). Figure 6 further demonstrates thickened fibrotic pericardium surrounding the myocardium on a heart cross section in IFN-γ–KO mice (Figure 6B) and a relative absence of the pericardial involvement in WT mice with a comparable myocarditis score (Figure 6A). IFN-γ–KO mice with increased pericardial fibrosis had reduced EDV (Figure 1D), but myocardial fibrosis in these mice had no association with EDV (Figure 1C).

Hemodynamic Effects of Pericarditis Not Related to Myocarditis

To test whether the hemodynamic changes consistent with constrictive/restrictive phenotype in the KO group were due to pericarditis but not the associated myocardial disease, we compared WT and KO mice matched for the severity of myocarditis. For this comparison, we chose WT mice that had the same histological scores of myocarditis as the KO mice with pericarditis described in the Table. Two KO mice were excluded from the comparison: 1 with no myocarditis (score of 0) and 1 with myocarditis score of 5 because none of the WT mice had this score. As a result, we compared 4 WT and 4 KO mice with similarly severe myocarditis with histological grades ranging from 3.5 to 4.5. When unmatched for myocarditis scores, the KO mice had a significantly greater percentage of myocardial fibrosis (data not shown). When matched for myocarditis scores, however, WT mice showed a significantly greater percentage of myocardial fibrosis (Figure 5B). Figure 2 demonstrates representative pressure-volume relations from immunized WT (Figure 2E) and KO (Figure 2F) mice with severe myocardial disease. Unlike WT mice, the KO mice developed pericarditis and had smaller LV volume, reduced stroke volume, and increased systolic and diastolic stiffness demonstrated by increased slopes of end-systolic and end-diastolic pressure-volume relations.

Despite comparable myocarditis scores and heart rate, the KO mice demonstrated increased heart weight (data not shown), reduced cardiac output (Figure 7A), and reduced LV volume (Figure 7G) and tended to have increased ejection fraction (Figure 7B). Consistent with the constrictive phenotype, the KO mice had significantly increased peak filling rate adjusted for EDV (Figure 7F) and increased systolic stiffness (Figure 7C). End-diastolic elastance, which was derived from multiple beats during preload reduction with the use of a monoexponential fit, was increased in both groups and tended to be higher in the KO mice, but the difference was not statistically significant (Figure 7I). Similarly, there was no significant difference in end-diastolic pressures between the 2 groups (Figure 7J). Because the lack of a significant difference in these 2 parameters was likely attributed to the fact that KO and WT mice operated over different volume ranges, we used a simple index of diastolic stiffness by comparing LV volumes at matched filling pressure of 7 mm Hg. This index was more sensitive in detecting increased diastolic stiffness in the KO mice (Figure 7K, 7L). Systolic function, as indicated by dP/dt_{max} and preload-recruitable stroke work, was reduced in both groups because of myocarditis but did not differ between the 2 genotypes and was therefore not affected by pericarditis (Figure 7D, 7E). Diastolic relaxation time constant (τ) was not significantly different between WT and KO groups (Figure 7H). Therefore, the increased τ in the group of IFN-γ–KO mice with pericarditis in the Table was more likely to be explained by the presence of severe myocarditis rather than pericardial disease. This conclusion is further supported by the lack of a relationship between pericardial fibrosis and τ (Figure 5D) and the presence of a strong positive association between myocardial fibrosis and τ in both KO and WT groups (Figure 5E, 5F, respectively). The latter observation points to the important role of myocardial fibrosis in prolongation of diastolic relaxation.

Discussion

This work presents the first description of an animal model of constrictive pericarditis. There have been few previous reports in the literature of pericarditis in animal models,

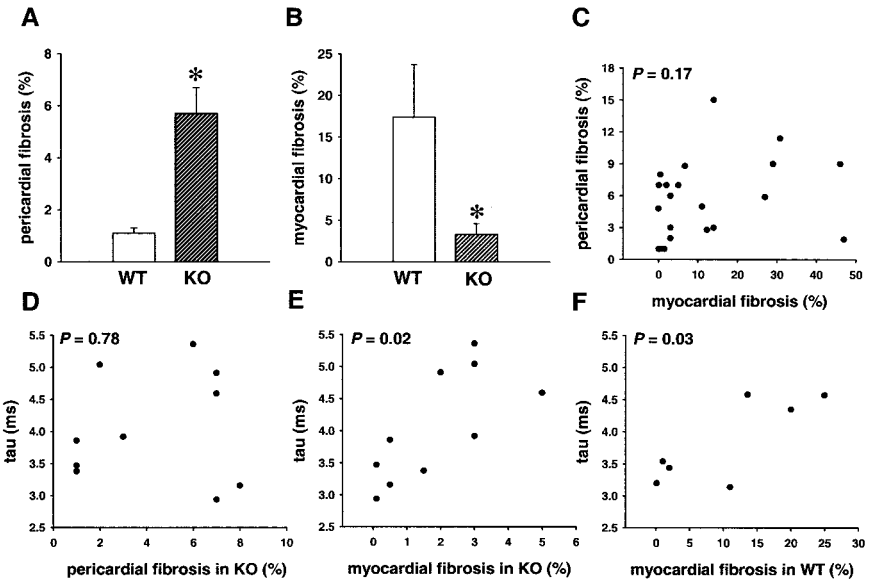

Figure 5. Pericardial and myocardial fibrosis in EAM in WT and IFN-γ–KO mice. A, Pericardial fibrosis in WT (n=9) and IFN-γ–KO (n=11) mice. B, Myocardial fibrosis in WT (n=4) and IFN-γ–KO (n=4) mice with matched histological scores of myocarditis. C, Lack of an association between myocardial and pericardial fibrosis in IFN-γ–KO mice. D, Pericardial fibrosis in IFN-γ–KO mice has no effect on diastolic relaxation time constant (τ). E and F, Significant positive association between myocardial fibrosis and τ in IFN-γ–KO (E) and WT (F) mice. In A and B, data are mean±SD. In C to F, each dot represents an individual mouse. Data are from day 21 after immunization. Percentage of fibrosis was assessed on heart sections with Masson's trichrome stain with the use of a microscope with a grid. Data represent percentages of the total cross section of the heart. *$P<0.05$, Student t test. In C, D, and E, probability value indicates significance of slope of the regression line.

including right ventricular perimyocarditis induced by coxsackie virus B3 infection in BALB/c mice,[10] pericarditis in sheep induced by injection of heat-killed staphylococci and Freund's adjuvant directly into the peritoneal cavity,[11] development of pancarditis in TGF-β1–KO mice,[12] and pericardiectomy-induced pericarditis in dogs and pigs.[13,14] None of these studies, however, demonstrated the presence of constriction. Constrictive pericarditis represents a hemodynamic syndrome, which is difficult to diagnose by morphological assessment of the pericardium. Recently, Talreja et al[15] demonstrated that constrictive pericarditis does not correlate with pericardial thickness, commonly used as an index of constriction. Measurements of pressure and volume signals using in vivo LV catheterization allowed us to characterize the constrictive phenotype in IFN-γ–KO mice. Pericardial constraint in these mice was associated with impaired diastolic filling, leading to reduced LV volumes and decreased cardiac output. Diastolic changes associated with pericarditis included increased peak filling rate adjusted for EDV compared with WT mice with comparable myocarditis scores. A monoexponentially derived index of diastolic stiffness (end-diastolic elastance) and end-diastolic pressures were not significantly elevated in the KO compared with WT mice with matched myocarditis scores. The KO mice with pericarditis, however, achieved the same diastolic pressures at significantly lower LV volumes, indicating increased chamber stiffness. It is likely that the lack of a significant difference in end-diastolic pressures was because the hearts with pericarditis were underfilled. Small LV volumes were due to both ejection to very small volumes associated with very high end-systolic elastance and the inability to fill because of constriction. Thus, the KO mice were typically operating over the lower portion of the end-diastolic pressure-volume relations curve. The combination of increased sensitivity to filling volume and steep end-systolic elastance was associated with increased pressure lability, resulting in reduced end-systolic pressures in the KO group (Table). To fully characterize the operating range in these hearts, it would have been beneficial to study the higher portion of the diastolic curve by additional volume loading. These measurements were not done in this study because of the sensitive hemodynamic state of mice with pericarditis.

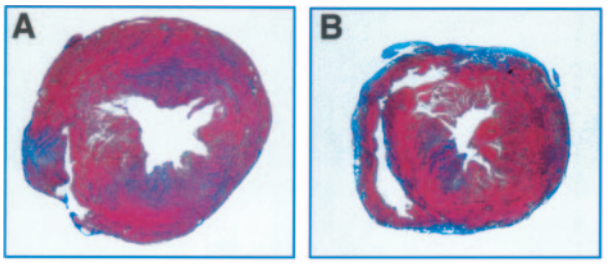

Figure 6. Heart cross sections from WT and IFN-γ–KO mice on day 21 after immunization. A, WT mouse with severe myocarditis and no constrictive pericarditis. B, IFN-γ–KO mouse with severe myocarditis and constrictive pericarditis. Note thickened fibrotic pericardium and small LV cavity. Masson's trichrome stain; magnification ×4.

Decreased cardiac performance associated with pericarditis was mainly due to diastolic dysfunction, because systolic function was largely preserved, as demonstrated by ejection fraction, increased end-systolic elastance and $dPdt_{max}$/EDV, and unchanged dP/dt_{max} and preload-recruitable stroke work compared with WT mice with the same degree of myocarditis. Diastolic dysfunction was characterized by the presence of typical pressure tracings and reduced deceleration time, resembling human cases of constrictive pericarditis. These hemodynamic phenomena were due to constriction rather than myocardial disease–related restriction because small LV volumes were associated with the presence of pericarditis but not the severity of myocarditis, and WT mice with severe myocarditis did not develop constrictive physiology. The relaxation time constant τ was unchanged, and peak filling rate adjusted for EDV was significantly increased in the KO group compared with the WT group matched for myocarditis scores, further confirming constrictive rather than restrictive physiology in the KO mice. We cannot completely exclude

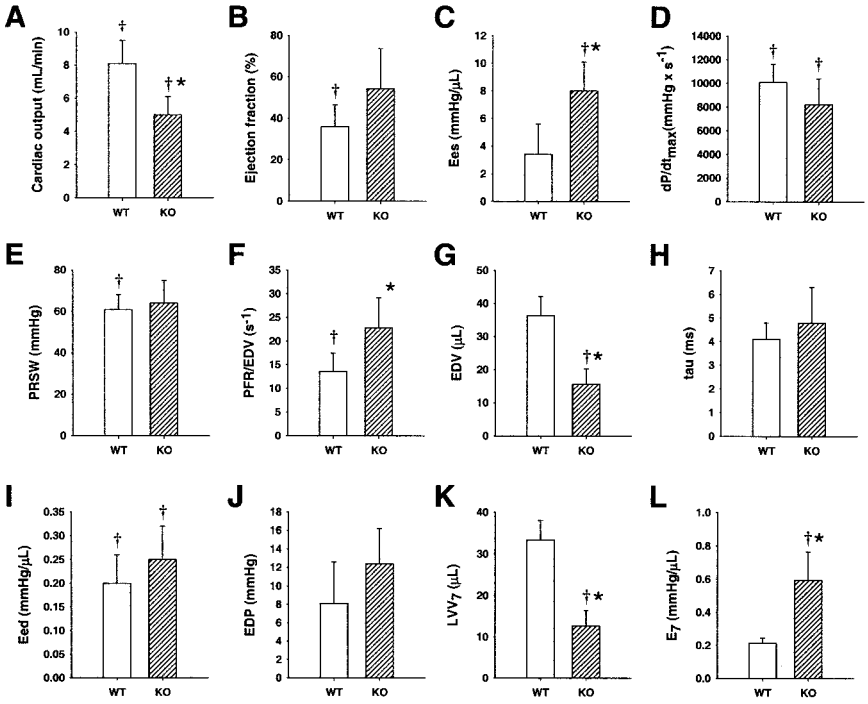

Figure 7. Hemodynamics in WT and IFN-γ–KO mice matched for myocarditis score. A, Cardiac output; B, ejection fraction; C, end-systolic elastance (Ees); D, dP/dt_{max}; E, preload-recruitable stroke work (PRSW); F, peak filling rate normalized to end-diastolic volume (PFR/EDV); G, EDV; H, isovolumic pressure relaxation time constant (τ); I, end-diastolic elastance (Eed); J, end-diastolic pressure (EDP); K, LV volume at filling pressure of 7 mm Hg (LVV_7); L, diastolic elastance at filling pressure of 7 mm Hg (E_7). Open bars represent data from WT mice, and striped bars represent data from KO mice. Data are mean±SD for 4 mice per group. *$P<0.05$ compared with WT with matched myocarditis scores; †$P<0.05$ compared with unimmunized controls (see Table for values in unimmunized controls), Student t test.

the possibility of residual restriction in IFN-γ–KO mice with pericarditis because most of the cases had an associated severe myocarditis. However, 1 of 6 mice with pericarditis in the study shown in the Table developed constrictive physiology but did not have any evidence of myocarditis (histological score of 0), which demonstrates that constrictive phenomena described in this work can occur independent of myocarditis. To our knowledge, this is the first report demonstrating inflammatory heart disease with predominantly diastolic dysfunction in an animal model.

Constrictive phenotype was characteristic of the acute phase of disease in IFN-γ–KO mice and represented the predominant phenotype on day 21 after immunization. The acute phase of disease was characterized by increased inflammation and fibrosis in the pericardium of IFN-γ–KO mice. Pericardial fibrosis was significantly associated with reduced EDV, and both pericardial inflammation and fibrosis correlated with decreased stroke volume, cardiac output, and stroke work (data not shown). At later time points, however, EDV in IFN-γ–KO mice increased, and there was no association between the presence of pericarditis and LV volumes (data not shown). Cardiac remodeling with dilatation at later time points may be due to the effects of myocardial inflammation and neurohormonal compensatory mechanisms in response to constriction.

Our work demonstrates that IFN-γ deficiency promotes the severity of pericarditis by leading to both greater inflammation and increased fibrosis in the pericardium. Neither pericardial fibrosis nor the degree of constriction correlated with the extent of myocardial inflammation in IFN-γ–KO mice, suggesting that the increased inflammatory response in these mice was not the sole determinant of the reactive pericardial fibrosis. Consistent with our observations, it has been reported that IFN-γ has antifibrotic activity and has been used to treat patients with idiopathic pulmonary fibrosis.[16] One potential mechanism through which the absence of IFN-γ promotes pericardial fibrosis involves upregulation of Th2-related cytokines, such as interleukin (IL)-4, IL-5, and IL-13. We previously reported that IFN-γ deficiency in EAM is associated with increased production of IL-4, IL-5, and IL-13.[8] The fibrogenic role of IL-4 and IL-13 has been demonstrated with the use of *Schistosoma mansoni*–induced fibrotic hepatic disease,[8,17] and blocking IL-4 prevented collagen deposition and fibrosis in a mouse model of scleroderma.[18] In vitro studies have further confirmed the stimulatory effects of IL-4 and suppressive effects of IFN-γ on fibroblast proliferation and collagen deposition.[19,20] It is therefore likely that Th2 cytokines are important for the development of fibrosis in the pericardium in EAM. Predominant Th2 responses in the absence of IFN-γ in EAM are also demonstrated by increased numbers of eosinophils in the pericardium. Eosinophils have been reported to participate in the development of fibrosis,[19,21] including the cardiac fibrosis associated with Loffler's endocarditis.[22]

In summary, this work describes a novel model of constrictive pericarditis, associated with the typical morphological features of pericarditis and a classic constrictive physiology. Because our work focuses on the acute phase of disease, future studies should address the effect of pericarditis on cardiac remodeling as well as morbidity and mortality at later time points. Future experiments are also needed to address the immune mechanisms as well as local signaling in the pericardium, including the mesothelial cell response to inflammatory stimuli and their role in the development of pericarditis. This model provides an opportunity to address these questions and also provides insights into the role of IFN-γ in the pathogenesis of pericarditis.

Acknowledgments

This work was supported by National Institutes of Health grants HL67290, HL70729, and AI51835.

References

1. Kabbani SS, LeWinter MM. Pericardial diseases. *Curr Treat Options Cardiovasc Med*. 2002;4:487–495.
2. Ling LH, Oh JK, Schaff HV, et al. Constrictive pericarditis in the modern era: evolving clinical spectrum and impact on outcome after pericardiectomy. *Circulation*. 1999;100:1380–1386.
3. Kabbani SS, LeWinter MM. Diastolic heart failure: constrictive, restrictive, and pericardial. *Cardiol Clin*. 2000;18:501–509.
4. Shiverick KL, Thomas LL, Alpert NR. Purification of cardiac myosin: application to hypertrophied myocardium. *Biochim Biophys Acta*. 1975; 393:124–133.
5. Georgakopoulos D, Kass D. Minimal force-frequency modulation of inotropy and relaxation of in situ murine heart. *J Physiol*. 2001;534: 535–545.
6. Matsubara H, Takaki M, Yasuhara S, et al. Logistic time constant of isovolumic relaxation pressure-time curve in the canine left ventricle: better alternative to exponential time constant. *Circulation*. 1995;92:2318–2326.
7. Afanasyeva M, Wang Y, Kaya Z, et al. Experimental autoimmune myocarditis in A/J mice is an interleukin-4-dependent disease with a Th2 phenotype. *Am J Pathol*. 2001;159:193–203.
8. Afanasyeva M, Wang Y, Kaya Z, et al. Interleukin-12 receptor/STAT4 signaling is required for the development of autoimmune myocarditis in mice by an interferon-gamma-independent pathway. *Circulation*. 2001; 104:3145–3151.
9. Little WC, Ohno M, Kitzman DW, et al. Determination of left ventricular chamber stiffness from the time for deceleration of early left ventricular filling. *Circulation*. 1995;92:1933–1939.
10. Matsumori A, Kawai C. Coxsackie virus B3 perimyocarditis in BALB/c mice: experimental model of chronic perimyocarditis in the right ventricle. *J Pathol*. 1980;131:97–106.
11. Leak LV, Ferrans VJ, Cohen SR, et al. Animal model of acute pericarditis and its progression to pericardial fibrosis and adhesions: ultrastructural studies. *Am J Anat*. 1987;180:373–390.
12. Kulkarni AB, Ward JM, Yaswen L, et al. Transforming growth factor-beta 1 null mice: an animal model for inflammatory disorders. *Am J Pathol*. 1995;146:264–275.
13. Page PL, Plumb VJ, Okumura K, et al. A new animal model of atrial flutter. *J Am Coll Cardiol*. 1986;8:872–879.
14. Loging JA, New RB, Baicu SC, et al. Effects of angiotensin type-I receptor blockade on pericardial fibrosis. *J Surg Res*. 1999;87:101–107.
15. Talreja DR, Edwards WD, Danielson GK, et al. Constrictive pericarditis in 26 patients with histologically normal pericardial thickness. *Circulation*. 2003;108:1852–1857.
16. Kalra S, Utz JP, Ryu JH. Interferon gamma-1b therapy for advanced idiopathic pulmonary fibrosis. *Mayo Clin Proc*. 2003;78:1082–1087.
17. Chiaramonte MG, Cheever AW, Malley JD, et al. Studies of murine schistosomiasis reveal interleukin-13 blockade as a treatment for established and progressive liver fibrosis. *Hepatology*. 2001;34:273–282.
18. Ong C, Wong C, Roberts CR, et al. Anti-IL-4 treatment prevents dermal collagen deposition in the tight-skin mouse model of scleroderma. *Eur J Immunol*. 1998;28:2619–2629.
19. Atamas SP, Luzina IG, Dai H, et al. Synergy between CD40 ligation and IL-4 on fibroblast proliferation involves IL-4 receptor signaling. *J Immunol*. 2002;168:1139–1145.
20. Duncan MR, Berman B. Gamma interferon is the lymphokine and beta interferon the monokine responsible for inhibition of fibroblast collagen production and late but not early fibroblast proliferation. *J Exp Med*. 1985;162:516–527.
21. Ando M, Miyazaki E, Fukami T, et al. Interleukin-4-producing cells in idiopathic pulmonary fibrosis: an immunohistochemical study. *Respirology*. 1999;4:383–391.
22. Seward JB, Tajik AJ. Primary cardiomyopathies: classification, pathophysiology, clinical recognition and management. *Cardiovasc Clin*. 1980; 10:199–230.

Novel Model of Constrictive Pericarditis Associated With Autoimmune Heart Disease in Interferon- γ–Knockout Mice

Marina Afanasyeva, Dimitrios Georgakopoulos, DeLisa Fairweather, Patrizio Caturegli, David A. Kass and Noel R. Rose

Circulation. 2004;110:2910-2917; originally published online October 25, 2004;
doi: 10.1161/01.CIR.0000147538.92263.3A
Circulation is published by the American Heart Association, 7272 Greenville Avenue, Dallas, TX 75231

Print ISSN: 0009-7322. Online ISSN: 1524-4539